CHAPTER 2

Broad-Scale Patterns of Insect and Disease Damage Across the United States From the National Insect and Disease Survey, 2022

Kevin M. Potter and
Jeanine L. Paschke

How to cite this chapter:

Potter, K.M.; Paschke, J.L. 2024. Broad-scale patterns of insect and disease damage across the United States from the national Insect and Disease Survey, 2022. In: Pandit, K.; Conkling, B.L., eds. Forest Health Monitoring: national status, trends, and analysis 2023. Gen. Tech. Rep. WO-105. Washington, DC: U.S. Department of Agriculture, Forest Service: 25–55. Chapter 2. https://doi.org/10.2737/WO-GTR-105-Chap2.

INTRODUCTION

U.S. law authorizes the U.S. Department of Agriculture, Forest Service to "conduct surveys to detect and appraise insect infestations and disease conditions and man-made stresses affecting trees and establish a monitoring system throughout the forests of the United States to determine detrimental changes or improvements that occur over time, and report annually concerning such surveys and monitoring" (FHP 2023). Forest insects and diseases have widespread ecological and economic impacts on forests across the United States and may represent the most serious threats to the Nation's forests (Logan and others 2003, Lovett and others 2016, Tobin 2015). Insects and diseases cause changes in forest structure and function, species succession, and biodiversity; these changes may be considered negative or positive depending on management objectives (Edmonds and others 2011).

Impacts of insects and diseases on forests vary from natural thinning to disruption of valued ecosystem processes due to tree mortality, but insects and diseases that kill trees are not necessarily the enemies of forests (Teale and Castello 2011). Disturbances such as insect and disease damage can sustain forest structures (Manion 2003, Zhang and others 2011) by facilitating a sanitation role, culling weak competitors, and releasing resources needed to support the growth of surviving trees (Teale and Castello 2011). Viewed in their full ecological context, some amount of insect- and disease-caused damage can therefore be considered "healthy." An important task for forest managers, pathologists, and entomologists is to recognize and distinguish between natural and excessive mortality, a task often informed by either ecologically based or commodity-based management objectives (Teale and Castello 2011).

Nearly all native tree species of the United States are affected by at least one injury-causing insect or disease agent, with native agents considerably less severe than nonnative ones (Potter and others 2019a). Additionally, the genetic integrity of several native tree species is highly vulnerable to the effects of nonnative diseases and insects (Potter and others 2019b). Introduced insects and diseases are of particular concern because they can extensively damage the biodiversity, ecology, and economy of affected areas (Brockerhoff and others 2006, Mack and others 2000). Few forests remain unaffected by invasive species, and their impacts to forest ecosystems are undeniable. These impacts can include wholesale changes in structures and function of ecosystems (Parry and Teale 2011).

Analyzing patterns of forest insect infestations, disease occurrences, forest declines, and related biotic stress factors is necessary to monitor the health of forested ecosystems and their potential impacts on forest structure, composition, biodiversity, and species distributions (Castello and others 1995). Examining insect pest occurrences and related stress factors from a landscape-scale perspective is useful, given the regional extent of many infestations and the large-scale complexity of interactions between host distribution, stress factors, and the development of outbreaks (Holdenrieder and others 2004, Liebhold and others 2013). One such landscape-scale approach is detecting geographic patterns of disturbance, allowing for the identification of areas at greater risk of significant ecological and economic impacts, and for selecting locations for more intensive monitoring and analysis. National Insect and Disease Survey (IDS) data (FHP 2023), coordinated by the Forest Service's Forest Health Protection (FHP) Program, provide an important source of information on forest disturbances and their causal agents across broad regions.

This chapter reports the area affected in 2022 by insect and disease mortality and defoliation-causing agents across all 50 States using IDS data collected by the Forest Service and its State partners. It further estimates the percentage of surveyed tree canopy cover area with insect- and disease-related mortality or defoliation within ecoregions across the United States and identifies statistically significant geographic hotspots of mortality or defoliation in the conterminous United States (CONUS).

METHODS

Data

The IDS data (FHP 2023) consist of information from low-altitude aerial survey and ground survey efforts by FHP and its partners in State agencies.[1] These data can be used to summarize insect and disease activity by regions in the CONUS, Alaska, and Hawaii (Potter 2012, 2013; Potter and Koch 2012; Potter and Paschke 2013, 2014, 2015a, 2015b, 2016, 2017, 2022, 2023; Potter and others 2018, 2019c, 2020a, 2021). IDS surveys across the CONUS in 2022 covered approximately 210.81 million ha encompassing both forested and unforested area (fig. 2.1). About 146.94 million ha of this area was forested, representing about 46.5 percent of the 315.99-million-ha tree canopy area of the CONUS. This was an increase of the tree-canopied area surveyed compared to 2020 and 2021 while similar to the amount surveyed in 2018 (46.6 percent) and 2019 (49.2 percent) (Potter and Paschke 2022, 2023; Potter and others 2020a, 2021). The 2022 data collection season, therefore, was more typical of those before the global COVID-19 (coronavirus) pandemic, which, in 2020, prevented many State partners and regional Forest Service personnel from conducting aerial survey flights because of risks posed by spending extended periods of time in the confined space of an aircraft. In Alaska, forest health specialists in 2022 surveyed 7.77 million ha across land cover types, of which about 5.85 million ha were forest and shrubland, or approximately 7.5 percent of the State's 77.78 million ha of total forest and shrubland. This was similar to the 7.2

[1] Analyses consist of data available from Forest Health Protection as of May 31, 2023.

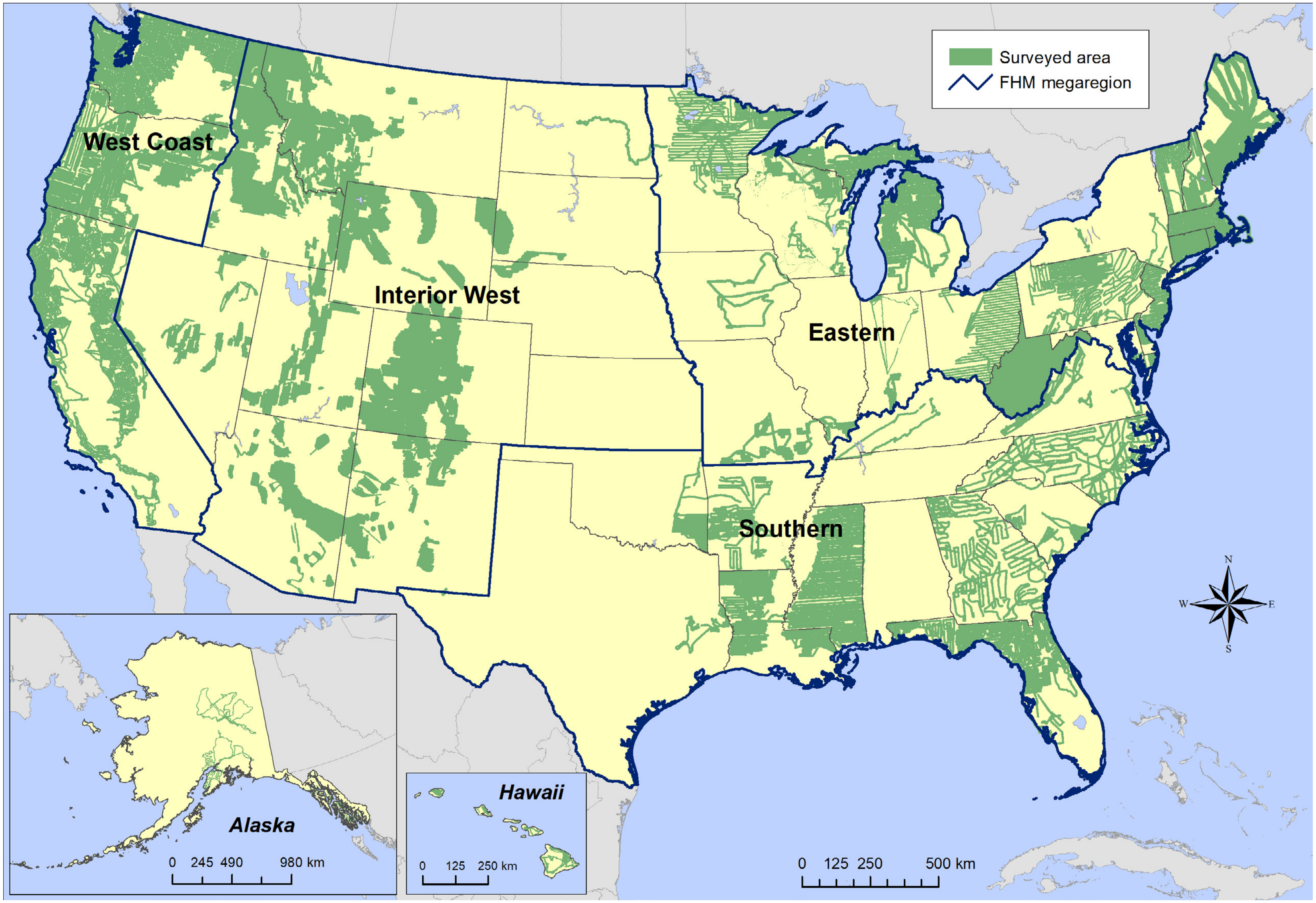

Figure 2.1—The extent of surveys for insect and disease activity conducted in the conterminous United States (CONUS), Alaska, and Hawaii in 2022. The blue lines delineate Forest Health Monitoring (FHM) megaregions in the CONUS. Note: Alaska and Hawaii are part of the West Coast megaregion, although their data are analyzed separately. Alaska and Hawaii are not shown to scale with map of the CONUS. (Data source: U.S. Department of Agriculture, Forest Service, Forest Health Protection)

percent surveyed in 2021 but more than the 2.8 percent surveyed in 2020 and less than the 12.7 percent and 10.8 percent surveyed in 2018 and 2019, respectively. In Hawaii, 2022 aerial survey efforts encompassed about 654 000 ha across all land cover types, including approximately 496 000 ha of tree canopy cover. This was about 57.6 percent of the total area of tree canopy, compared to 65.5 percent in 2021, 60.3 percent in 2020, 63.9 percent in 2019, and 69.4 percent in 2018.

The Digital Mobile Sketch Mapping (DMSM) platform includes tablet hardware, software, and data support processes allowing trained aerial surveyors in light aircraft, as well as ground observers and those using other remote sensing data, to record forest disturbances and their causal agents. DMSM enhances the quality and quantity of forest health data by integrating with remote sensing platforms (FHP 2019). Geospatial data collected with DMSM are stored in the national IDS database. DMSM includes both polygon geometry, used for damage areas where boundaries are discrete and obvious, and point geometry, used for small clusters of damage where size and shape of the damage are less important than recording the location. Good examples of insects and diseases for which point data are utilized include sudden oak death (caused by the pathogen *Phytophthora ramorum*), southern pine beetle (*Dendroctonus frontalis*), and some types of bark beetle damage in the West. For analyses in this report, these points were assigned an area of 0.8 ha (about 2 acres). Additionally, DMSM allows for the use of grid cells (240-, 480-, 960-, or 1920-m resolution) to estimate the percentage of trees affected by damages that may be widespread and diffuse, such as those associated with spongy moth (*Lymantria dispar*), emerald ash borer (*Agrilus planipennis*), and hurricanes (an abiotic disturbance not included in this chapter). When calculating the total areas affected by each damage agent, this study used the entire areas of these grid cells (e.g., 240-m cell = 5.76 ha).

The DMSM platform allows surveyors to both define the extent of an area experiencing damage and estimate the percent range of the area affected within polygons (Berryman and McMahan 2019). While additional validation is required, this relatively new method is expected to increase the accuracy of derived damage metrics because it potentially corrects for previous areal overestimation caused by "lassoing" areas of undamaged trees into large areas of damage (Coleman and others 2018, Slaton and others 2021). IDS analysis chapters in Forest Health Monitoring (FHM) reports before 2019 did not incorporate derived damage estimates beyond the areal footprint damage with mortality or defoliation polygon boundaries. However, these are now possible because of the inclusion of damage percentage estimates within polygons (see Analyses below).

The IDS database identifies areas with mortality or defoliation caused by biotic or abiotic factors, though the focus of this set of analyses is insect and disease activity. A visual interpreter might consider a pathogen or insect to be a mortality-causing agent in one location and a defoliation-causing agent in another, depending on the level of damage to the forest in an area, the specific host-pest relationship, and the convergence of other stress factors such as drought. In some cases, identified agents of mortality or defoliation are complexes of multiple agents summarized under an impact label related to a specific host tree species (e.g., "beech bark disease complex" or "yellow-cedar decline"). In other cases, one or more agents (for example, ash yellows (caused by the *Candidatus Phytoplasma fraxini* bacterium), ash rust (*Puccinia sparganioides*), and verticillium wilt (*Verticillium albo-atrum*) in ash (*Fraxinus* spp.)) may cause stress to a tree that may ultimately increase its susceptibility to another agent to which the damage is attributed (in this example by emerald ash borer). Differences in data collection, attribute recognition, and coding procedures among States and regions can complicate data analysis and interpretation of results.

Some important mortality and defoliation agents have not been easily detected or thoroughly quantified through aerial detection and other remote sensing methods. This includes (1) insects such as emerald ash borer and hemlock woolly adelgid (*Adelges tsugae*); (2) diseases such as laurel wilt (*Harringtonia lauricola*, previously *Raffaelea lauricola*), Dutch elm disease (*Ophiostoma novo-ulmi*), white pine blister rust (*Cronartium ribicola*), and thousand cankers disease (*Geosmithia morbida*); and (3) mortality complexes (such as oak decline). (Recent efforts, however, have successfully used remotely sensed data to map damage caused by hemlock woolly adelgid, laurel wilt, and emerald ash borer in urban settings (Abdulridha and others 2018, Hanavan and others 2015, Pontius and others 2017).) Such pests may attack hosts that are widely dispersed throughout forests with high tree species diversity or may cause mortality or defoliation that is otherwise difficult to perceive.

A comparison of aerial survey data by four aerial observers with ground presence/absence observations found the accuracy of aerial survey data exceeded 70 percent and damage type observations for tree mortality and defoliation had high levels of accuracy. However, the comparison further showed the accuracy declined for severity estimates and as specificity for observations went from the genus to the species level for tree species and damage agents (Coleman and others 2018). Recent long-term analyses of these data highlight insects as more widely detected agents of mortality compared to diseases, with bark beetles consistently the most important mortality agents across regions and time (Potter and others 2020b). (These results may be somewhat skewed toward insects because the visible signatures of insect damage are easier for IDS surveyors to detect.)

Analyses

This study generated three sets of indicators of forest insect and disease damage for 2022: (1) a series of tables reporting the most widely detected mortality and defoliation agents nationally and regionally, (2) estimates of the percentage of surveyed tree canopy cover area with insect- and disease-related mortality or defoliation within ecoregions across the United States, and (3) statistically significant geographic hotspots of mortality or defoliation in the CONUS.

The first analysis used the 2022 mortality and defoliation polygons to identify the select mortality and defoliation agents and complexes causing damage on >5000 ha of forest in the CONUS that year. Similarly, lists were generated for the five most widely reported mortality and defoliation agents and complexes within each of the four FHM megaregions in the CONUS (West Coast, Interior West, Eastern, and Southern), as well as separately for Alaska and Hawaii when data were available. Because of the insect and disease aerial sketch-mapping process (i.e., mostly digitization of polygons by a human interpreter aboard an aircraft), all quantities are approximate "footprint" areas for each agent or complex. These delineate areas of visible damage within which the agent or complex is present. Unaffected trees may exist within the footprint, and the amount of damage within the footprint is not necessarily reflected in the estimates of forest area affected. Additionally, the sum of areas affected by all individual agents and complexes is not equal to the total affected area because of overlapping polygons and because of the reporting of multiple agents per polygon in some situations.

The second set of analyses used the IDS data for 2022 to more directly estimate the impacts of insect- and disease-related mortality and defoliation on U.S. forests within a spatial context. These results are reported in a set of figures describing, within ecoregions across the United States, the percentage of surveyed tree canopy cover area with insect- and disease-related mortality or defoliation. Specifically, as an indicator of the extent of damaging insect and disease agents, this study summarized the percentage of surveyed tree canopy cover area experiencing mortality or defoliation for ecoregions within the CONUS and Hawaii, and for surveyed forest and shrubland in Alaska ecoregions. This is a change from FHM reports before 2019, which reported the percentage of regions *exposed to* mortality and defoliating agents based only on the footprint with mortality or defoliation polygon boundaries (masked by forest cover) because information on the percentage of damage within polygons was not yet consistently available. As noted above, DMSM now allows surveyors to both define the extent of an area experiencing damage and estimate percent range of the area within the polygon affected (specifically, 1–3 percent, 4–10 percent, 11–29 percent, 30–50 percent, and >50 percent). Generating an adjusted estimate of the area affected by each mortality or defoliation agent detection is now possible by multiplying the area of damage within each polygon (after masking by tree canopy cover) by the midpoint of the estimated percent-affected range (Berryman and McMahan 2019). These individual estimates can be summed for all polygons within an ecoregion and divided by the total surveyed tree canopy cover area within the ecoregion to generate an estimate of the percentage of its canopy cover area affected by defoliating or mortality-causing agents. (DMSM point data are also included in this estimate. Surveyors have the option to estimate the number of trees affected at a point and are required to assign an area value associated with each point, which is assumed to be 100 percent affected by its mortality or defoliation agent. For simplicity, each point was transformed into a 2-acre (0.809-ha) polygon. These areas for all the points in an ecoregion were then added to the polygon-adjusted affected area estimates for the ecoregion.)

This study calculated the percentage of surveyed tree canopy area with mortality or defoliation within each of the 190 ecoregion sections in the CONUS (Cleland and others 2007) and, similarly, summarized mortality and defoliation data for each of the 32 ecoregion sections in Alaska (Spencer and others 2002). For Hawaii, the percentage of surveyed tree canopy area affected by mortality and defoliation agents in 34 ecoregion subunits within the archipelago was calculated (Potter 2023). Statistics were not calculated for ecoregions in the CONUS and Hawaii with ≤5 percent of the tree canopy cover area surveyed, nor in Alaska with ≤2.5 percent of the forest and shrubland area surveyed.

To represent tree canopy for the CONUS and Hawaii, tree canopy data were resampled to 240 m from a 30-m raster dataset that estimates percentage of tree canopy cover (0–100 percent) for each grid cell; this dataset was generated from the 2011 National Land Cover Database (NLCD) (Homer and others 2015) through a cooperative project between the Multi-Resolution Land Characteristics Consortium and the Forest Service Geospatial Technology and Applications Center (GTAC) (Coulston and others 2012). Any cell with >0 percent tree canopy cover was treated as forest. Comparable tree canopy cover data were not available for Alaska, so a 240-m-resolution layer of forest and shrub cover was instead created from the 2011 NLCD.

Finally, the third set of analyses used the Spatial Association of Scalable Hexagons (SASH) analytical approach to identify statistically significant geographic hotspots of mortality or defoliation in the CONUS. This method identifies locations where ecological phenomena occur at greater or lower frequency than expected by random chance and is based on a sampling frame optimized for spatial neighborhood analysis, adjustable to the appropriate spatial resolution, and applicable to multiple data types (Potter and others 2016). Specifically, it encompasses two steps: first, dividing an analysis area into scalable equal-area hexagonal cells within which data are aggregated and, second, identifying statistically significant geographic clusters of hexagonal cells within which mean values are greater or less than those expected by chance. Separate Getis-Ord (Gi^*) hotspot analyses (Getis and Ord 1992) in

ArcMap® 10.3 (ESRI 2017) identified clusters of both mortality- and defoliation-causing agents across the CONUS. The low density of survey data in 2022 from Alaska and the small spatial extent of Hawaii (fig. 2.1) precluded the use of Getis-Ord *Gi** hotspot analyses in these areas.

The units of analysis were 9,810 hexagonal cells, each approximately 834 km^2 in area, generated in a lattice across the CONUS using intensification of the Environmental Monitoring and Assessment Program (EMAP) North American hexagon coordinates (White and others 1992). These coordinates are the foundation of a sampling frame in which a hexagonal lattice was projected onto the CONUS by centering a large base hexagon over the region (Reams and others 2005, White and others 1992). This base hexagon can be subdivided into many smaller hexagons, depending on sampling needs, and serves as the basis of the plot sampling frame for the Forest Service's Forest Inventory and Analysis (FIA) Program (Reams and others 2005). Importantly, hexagons maintain equal areas across the study region regardless of the degree of intensification of the EMAP hexagon coordinates. In addition, hexagons are compact and uniform in their distance to the centroids of neighboring hexagons, meaning a hexagonal lattice has a higher degree of isotropy (uniformity in all directions) than does a square grid (Shima and others 2010). These are convenient and highly useful attributes for spatial neighborhood analyses. These scalable hexagons are independent of geopolitical and ecological boundaries, avoiding the possibility of different sample units (such as counties, States, or watersheds) encompassing vastly different areas (Potter and others 2016). The 834-km^2 hexagons are a manageable size for making monitoring and management decisions in analyses that are national in extent (Potter and others 2016).

Next, the Getis-Ord G_i^* statistic was used to identify clusters of hexagonal cells within which the percentage of surveyed tree canopy area with mortality or defoliation was higher than expected by chance. This statistic allows for the decomposition of a global measure of spatial association into its contributing factors, by location, and is therefore particularly suitable for detecting instances of nonstationarity in a dataset, such as when spatial clustering is concentrated in one subregion of the data (Anselin 1992). Hexagons were excluded if they contained ≤5 percent tree canopy cover or if ≤1 percent of the tree canopy cover was surveyed in 2022.

The Getis-Ord G_i^* statistic for each hexagon summed differences between mean values in a local sample, determined by a moving window consisting of the hexagon and its 18 first- and second-order neighbors (the 6 adjacent hexagons and the 12 additional hexagons contiguous to those 6) and a global mean. The G_i^* statistic was standardized as a *z*-score with a mean of 0 and a standard deviation of 1, with values >1.96 representing significant (p <0.025) local clustering of high values and values <-1.96 representing significant clustering of low values (p <0.025), since 95 percent of observations under a normal distribution should be within approximately two (exactly 1.96) standard deviations of the mean (Laffan 2006). In other words, a G_i^* value of 1.96 indicates the local mean of the percentage of forest exposed to mortality- or defoliation-causing agents for a hexagon and its 18 neighbors is approximately 2 standard deviations greater than the mean expected in the absence of spatial clustering, while a G_i^* value of -1.96 indicates the local mortality or defoliation mean for a hexagon and its 18 neighbors is approximately 2 standard deviations less than the mean expected in the absence of spatial clustering. Values between -1.96 and 1.96 have no statistically significant concentration of high or low values. In other words, when a hexagon has a G_i^* value between -1.96 and 1.96, mortality or defoliation damage within it and its 18 neighbors is not statistically different from a normal expectation. As described in Laffan (2006), it is calculated as:

$$G_i^*(\boldsymbol{d}) = \frac{\sum_j w_{ij}(d)x_j - W_i^*\bar{x}^*}{s^*\sqrt{\frac{(ns_{1i}^*) - W_i^{*2}}{n-1}}}$$

where

G_i^* = the local clustering statistic (in this case, for the target hexagon)

i = the center of local neighborhood (the target hexagon)

d = the width of local sample window (the target hexagon and its first- and second-order neighbors)

x_j = the value of neighbor j

w_{ij} = the weight of neighbor j from location i (all the neighboring hexagons in the moving window were given an equal weight of 1)

n = number of samples in the dataset (the 4,178 hexagons containing >5-percent tree cover and with at least 1 percent of the canopy cover surveyed)

W_i^* = the sum of the weights

s^*_{1i} = the number of samples within d of the central location (19: the focal hexagon and its 18 first- and second-order neighbors)

$\bar{x}^*$= mean of whole dataset (in this case, the 4,178 hexagons)

s^* = the standard deviation of whole dataset (for the 4,178 hexagons)

Note that the -1.96 and 1.96 threshold values are not exact because the correlation of spatial data violates the assumption of independence required for statistical significance (Laffan 2006). The Getis-Ord approach does not require the input data to be normally distributed because the local G_i^* values are computed under a randomization assumption, with G_i^* equating to a standardized z-score that asymptotically tends to a normal distribution (Anselin 1992). The z-scores are reliable, even with skewed data, if the distance band used to define the local sample around the target observation is large enough to include several neighbors for each feature (ESRI 2017).

RESULTS AND DISCUSSION

Conterminous United States Mortality

In 2022, surveyors identified 52 mortality-causing agents and complexes across the CONUS on about 3.33 million ha. This represents approximately the land area of Connecticut and Massachusetts combined. Of the agents in the national IDS database for the year, 19 were detected on >5000 ha. This compares to 60 agents and complexes detected on 2.21 million ha in 2021 and 45 detected on 1.17 million ha in 2020 (Potter and Paschke 2022, 2023). The 2021 and 2022 figures are more consistent with those typical of data collection before the COVID-19 pandemic, e.g., 2.69 million ha of damage associated with 58 agents and complexes in 2019 (Potter and others 2021).

The most widely detected mortality agent in 2022 was fir engraver (*Scolytus ventralis*), identified on 1.36 million ha, followed by emerald ash borer, found on about 582 000 ha, and western pine beetle (*D. brevicomis*), on approximately 303 000 ha (table 2.1). These represented, respectively, about 41, 17, and 9 percent of the total CONUS mortality area. Fir engraver was the most widely detected mortality agent in 2020, while emerald ash borer was more widely detected in 2021 (Potter and Paschke 2022, 2023). Worth noting, however, is the challenging nature of mapping emerald ash borer damage via aerial surveys, including the differentiation of damage occurrence between years and the fact that agents other than emerald ash borer damage ash species.

Table 2.1—Mortality agents and complexes affecting >5000 ha in the conterminous United States during 2022

Agents/complexes causing mortality, 2022	Area (ha)[a]
Fir engraver	1 356 411
Emerald ash borer	581 963
Western pine beetle	302 932
Flatheaded fir borer	259 722
Pinyon ips	172 475
Unknown bark beetle	136 751
Eastern larch beetle	123 122
Douglas-fir beetle[b]	116 550
Mountain pine beetle	108 575
Unknown	87 179
Balsam woolly adelgid	41 911
Western balsam bark beetle	36 681
Spruce beetle	33 988
Subalpine fir decline	26 127
Ips engraver beetles	25 844
Oak decline	25 391
Jeffrey pine beetle	16 638
Spongy moth	6632
Southern pine beetle	5635
Other (33)	15 132
Total, all mortality agents	3 326 087

[a] All values are "footprint" areas for each agent or complex. The sum of the individual agents is not equal to the total for all agents due to the reporting of multiple agents per polygon.

[b] In the Interior West, this is primarily damage on ponderosa pines. The group of bark beetles is known and varied but not distinguishable from the air. Regions have characterized it as "Southwest bark beetle complex" consisting mainly of damage caused by roundheaded pine beetle, western pine beetle, and ips beetles.

Six other agents were detected on >100 000 ha. These were flatheaded fir borer (*Phaenops drummondi*) on 260 000 ha, pinyon ips (*Ips confusus*) on 172 000 ha, "unknown bark beetle"[2] on 137 000 ha, eastern larch beetle (*D. simplex*) on 123 000 ha, Douglas-fir beetle (*D. pseudotsugae*) on 117 000 ha, and mountain pine beetle (*D. ponderosae*) on 109 000 ha (table 2.1). Meanwhile, mortality from the 15 IDS agents constituting the western bark beetle group (table 2.2) accounted for two-thirds of all the 2022 mortality area across the CONUS (2.21 million ha in the West). Six of the 10 most widely detected mortality agents and complexes belonged to this group.

The CONUS portion of the West Coast FHM megaregion had the largest area of detected mortality within the area surveyed, about 2.02 million ha linked to 22 agents and complexes (table 2.3). Almost two-thirds of this area (64.3 percent) was associated with fir engraver (1.30 million ha). Three other bark beetles also were detected on large areas: western pine beetle on 302 000 ha (15.0 percent of the total), mountain pine beetle on 90 000 ha (4.5 percent), and Douglas-fir beetle on 69 000 ha (3.4 percent). An additional 12.9 percent of the total megaregion mortality area (260 000 ha) was attributed to flatheaded fir borer.

Table 2.2—Beetle taxa included in the "western bark beetle" group in 2022

Western bark beetle mortality agents	
Cedar and cypress bark beetles	*Phloeosinus* spp.
Douglas-fir beetle	*Dendroctonus pseudotsugae*
Douglas-fir engraver	*Scolytus unispinosus*
Fir engraver	*Scolytus ventralis*
Ips engraver beetles	*Ips* spp.
Jeffrey pine beetle	*Dendroctonus jeffreyi*
Mountain pine beetle	*Dendroctonus ponderosae*
Pine engraver	*Ips pini*
Pinyon ips	*Ips confusus*
Roundheaded pine beetle	*Dendroctonus adjunctus*
Silver fir beetle	*Pseudohylesinus sericeus*
Spruce beetle	*Dendroctonus rufipennis*
Unknown bark beetle[a]	—
Western balsam bark beetle	*Dryocoetes confusus*
Western pine beetle	*Dendroctonus brevicomis*

[a] In the Interior West, this is primarily damage on ponderosa pines. The group of bark beetles is known and varied but not distinguishable from the air. Regions have characterized it as "Southwest bark beetle complex" consisting mainly of damage caused by roundheaded pine beetle, western pine beetle, and ips beetles.

[2] The unknown bark beetle agent encompasses a group of known and varied bark beetles, impossible to distinguish using IDS data, that primarily damage ponderosa pine (*Pinus ponderosa*) forests. This also has been characterized as "Southwest bark beetle complex" consisting mainly of damage caused by roundheaded pine beetle (*D. adjunctus*), western pine beetle, and ips beetles.

Table 2.3—The top five mortality agents or complexes for each Forest Health Monitoring megaregion and for Alaska and Hawaii in 2022

Mortality agents and complexes, 2022	Area (ha)[a]
Eastern	
Emerald ash borer	581 900
Eastern larch beetle	123 122
Unknown	27 294
Oak decline	25 391
Spongy moth	6632
Other mortality agents (23)	15 176
Total, all mortality agents and complexes	779 374
Interior West	
Pinyon ips	171 784
Unknown bark beetle[b]	129 559
Fir engraver	58 850
Douglas-fir beetle	45 845
Spruce beetle	33 206
Other mortality agents (14)	91 387
Total, all mortality agents and complexes	516 734
Southern	
Ips engraver beetles	9365
Southern pine beetle	1555
Douglas-fir beetle[c]	1376
Unknown	468
Unknown bark beetle[c]	262
Other mortality agents (3)	102
Total, all mortality agents and complexes	13 128

Mortality agents and complexes, 2022	Area (ha)[a]
West Coast (CONUS)	
Fir engraver	1 297 561
Western pine beetle	301 626
Flatheaded fir borer	259 722
Mountain pine beetle	89 773
Douglas-fir beetle	69 329
Other mortality agents (17)	138 374
Total, all mortality agents and complexes	2 016 851
Alaska	
Spruce beetle	19 740
Yellow-cedar decline	4725
Northern spruce engraver	338
Aspen running canker	20
Unknown	15
Other mortality agents (1)	2
Total, all mortality agents and complexes	24 840
Hawaii	
Unknown[d]	36 415
Total, all mortality agents and complexes	36 415

[a] The total area affected by other agents is listed at the end of each section. All values are "footprint" areas for each agent or complex. The sum of the individual agents is not equal to the total for all agents due to the reporting of multiple agents per polygon.

[b] In the Interior West, this is primarily damage on ponderosa pines. The group of bark beetles is known and varied but not distinguishable from the air. Regions have characterized it as "Southwest bark beetle complex" consisting mainly of damage caused by roundheaded pine beetle, western pine beetle, and ips beetles.

[c] Personnel from Forest Service Region 3 (Southwestern Region) conducted surveys into southwestern Texas (Region 8 [Southern Region]) because of extended damage in the Guadalupe Mountains which included Douglas-fir beetle and "unknown bark beetle" damage on ponderosa pines (see note b).

[d] Most of the mortality recorded in Hawaii is coded as "unknown" mortality on ʻōhiʻa lehua. Damage is likely attributed to rapid ʻōhiʻa death but has not been confirmed in all cases.

Within the CONUS portion of the West Coast megaregion, ecoregion sections in eastern and northern California and southwestern Oregon experienced high levels of mortality (2.0–5.0 percent of surveyed tree canopy cover) (fig. 2.2). Specifically, both M261E–Sierra Nevada and M261A–Klamath Mountains had 3.1 percent mortality within surveyed areas. In the former, fir engraver caused extensive mortality in California red fir (*Abies magnifica* var. *shastensis*) and white fir (*A. concolor*) stands. In the latter, flatheaded fir borer caused mortality in Douglas-fir (*Pseudotsuga menziesii*) stands, western pine beetle affected ponderosa pine stands, and fir engraver killed white fir. Meanwhile, fir engraver in white fir, California red fir, noble fir (*A. procera*), and grand fir (*A. grandis*) resulted in 2.8 percent mortality of the surveyed tree canopy cover of M261D–Southern Cascades. Neighboring ecoregion sections also had high mortality (1.0–2.5 percent of surveyed area): M261G–Modoc Plateau (2.4 percent) and M261B–Northern California Coast Ranges (1.7 percent).

Not surprisingly, the CONUS portion of the West Coast megaregion encompassed several hotspots of mortality density, including one of very high density in southwestern Oregon and four of high density across northern and eastern California (fig. 2.3). An additional hotspot of high mortality density was centered on M332G–Blue Mountains and 342H–Blue Mountain Foothills in east-central Oregon, where surveyors detected extensive fir engraver damage in fir forests, as well as some ponderosa pine mortality attributed to western pine beetle and lodgepole pine (*P. contorta*) mortality attributed to mountain pine beetle.

With about 800 000 ha of damage, the Eastern FHM megaregion in 2022 had the second largest area on which mortality agents and complexes were detected (table 2.3). A total of 28 agents and complexes were inventoried in the megaregion. As in recent years, a large majority of the mortality (74.7 percent in 2022 and 86.2 percent in 2021) was associated with emerald ash borer, detected on 582 000 ha. Other widespread mortality agents identified in the megaregion were eastern larch beetle (123 000 ha, 15.8 percent of the total), oak decline (25 000 ha, 3.3 percent), and spongy moth (7000 ha, 0.9 percent).

Emerald ash borer caused the extremely high levels of mortality (>5.0 percent) of surveyed canopy cover area in ecoregion sections of Iowa, Minnesota, and Wisconsin: 251B–North Central Glaciated Plains (31.2 percent), 222L–North Central U.S. Driftless and Escarpment (9.5 percent), and 222M–Minnesota and Northeast Iowa Morainal-Oak Savannah (7.6 percent) (fig. 2.2). The affected host species were white, green, and black ash (*F. americana, F. pennsylvanica*, and *F. nigra*). These ecoregion sections, along with 251C–Central Dissected Till Plains, were the location of a hotspot of extremely high and very high mortality density (fig. 2.3).

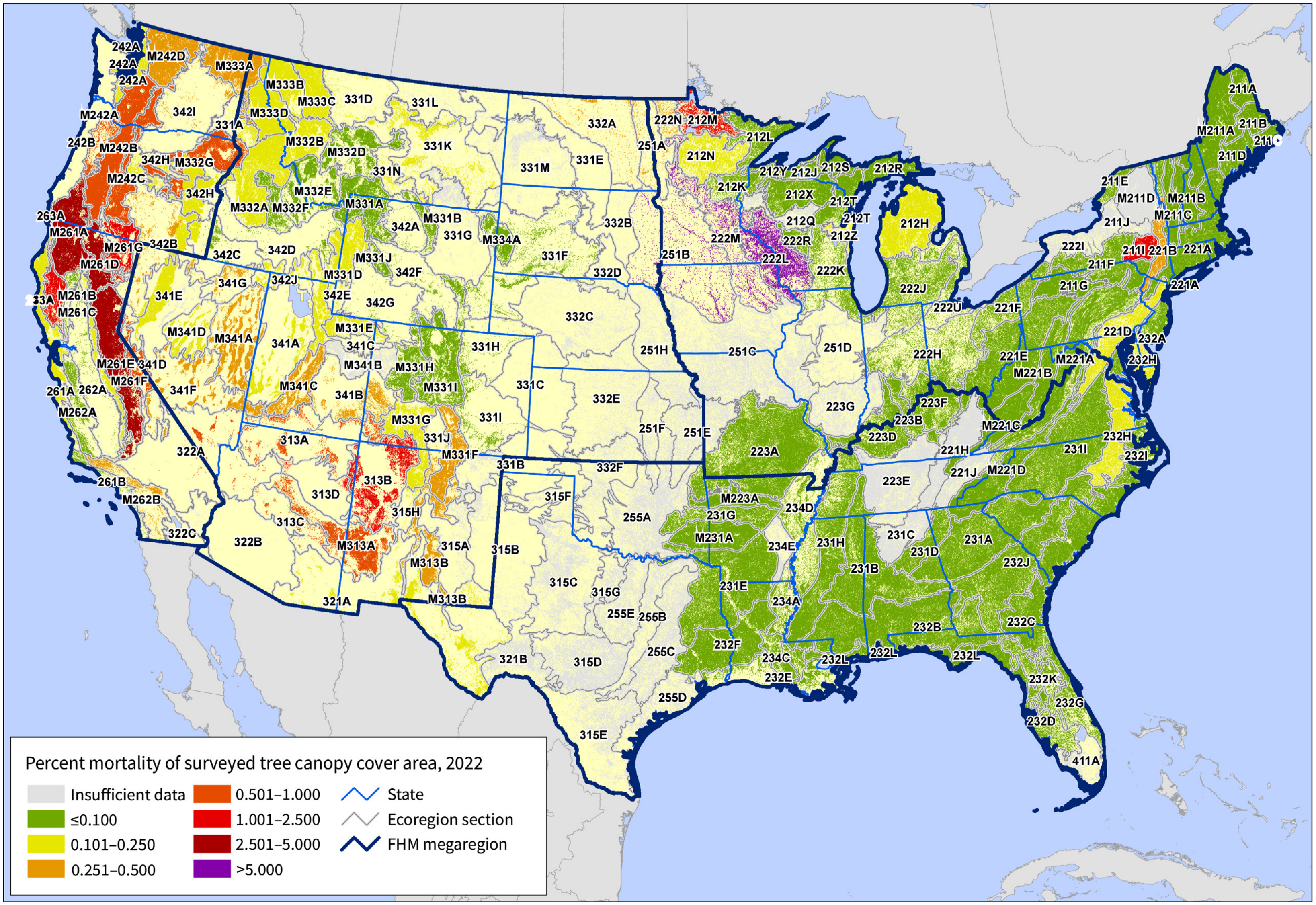

Figure 2.2—The percentage of surveyed tree canopy cover area with insect and disease mortality, by ecoregion section within the conterminous United States, for 2022. The gray lines delineate ecoregion sections (Cleland and others 2007), and dark blue lines delineate Forest Health Monitoring megaregions. The 240-m tree canopy cover is based on data from a cooperative project between the Multi-Resolution Land Characteristics Consortium (Coulston and others 2012) and the Forest Service Geospatial Technology and Applications Center using the 2011 National Land Cover Database. (Data source: U.S. Department of Agriculture, Forest Service, Forest Health Protection)

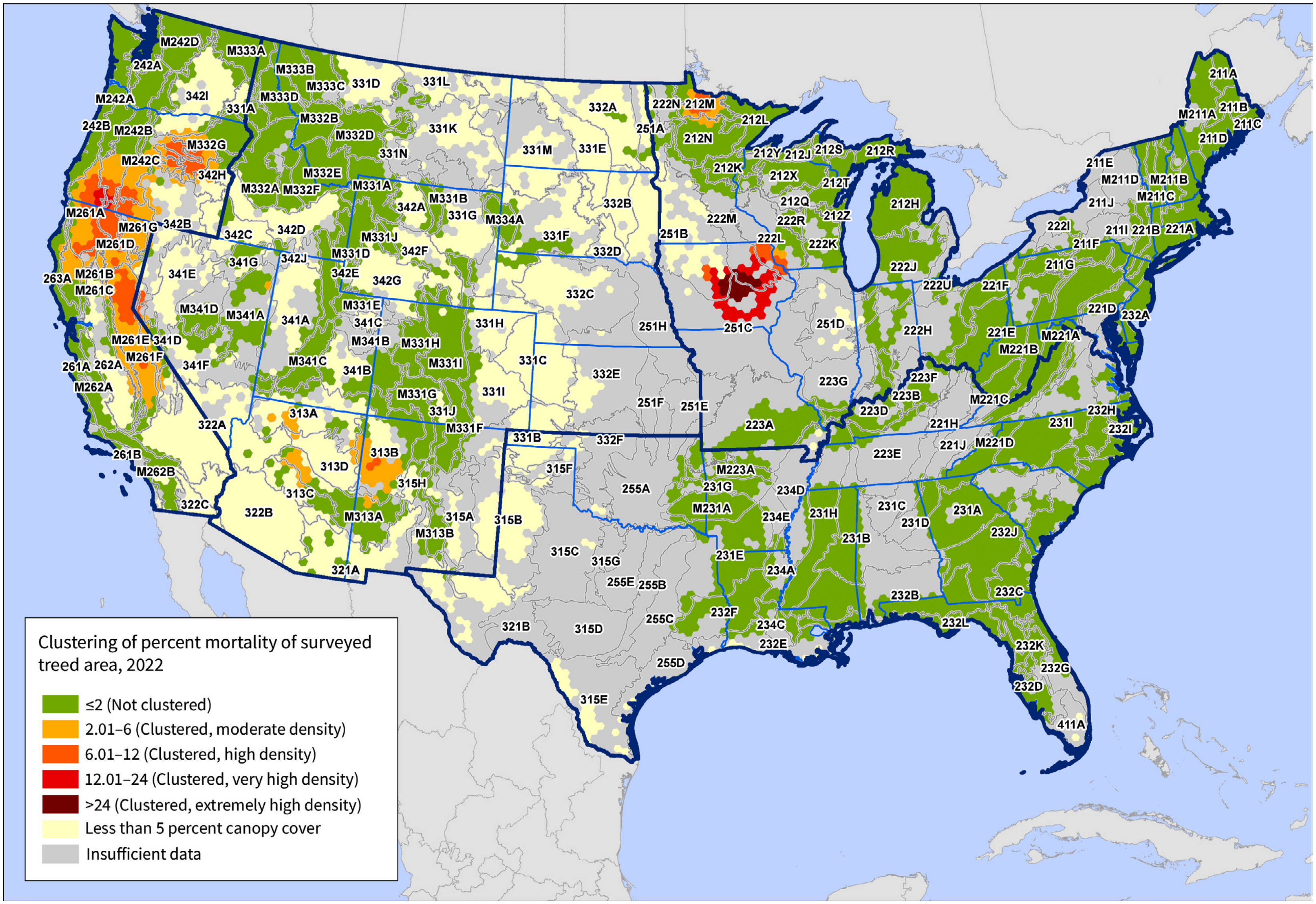

Figure 2.3—Hotspots of percentage of surveyed tree canopy cover area with insect and disease mortality in 2022 for the conterminous United States by hexagons containing >5 percent tree canopy cover. Values are Getis-Ord Gi scores, with values >2 representing significant clustering of high mortality occurrence densities and values <-2 representing significant clustering of low mortality occurrence densities. The gray lines delineate ecoregion sections (Cleland and others 2007), and dark blue lines delineate Forest Health Monitoring megaregions. Tree canopy cover is based on data from a cooperative project between the Multi-Resolution Land Characteristics Consortium (Coulston and others 2012) and the Forest Service Geospatial Technology and Applications Center using the 2011 National Land Cover Database. (Data source: U.S. Department of Agriculture, Forest Service, Forest Health Protection)*

Meanwhile, the 212M–Northern Minnesota and Ontario ecoregion section experienced 2.1 percent mortality of surveyed tree canopy cover because of an ongoing eastern larch beetle outbreak in tamarack (*Larix laricina*) (fig. 2.2). This corresponded with a hotspot of high and moderate mortality density (fig. 2.3). Additionally, emerald ash borer damage in northern New York resulted in 1.2 percent mortality of surveyed canopy cover in 211I–Catskill Mountains and 0.4 percent mortality in 221B–Hudson Valley.

Surveyors in the Interior West megaregion during 2022 identified damage from 19 mortality agents and complexes across 517 000 ha (table 2.3). The most widespread was pinyon ips, detected on 172 000 ha, or 33.2 percent of all the mortality in the region. This was followed by the unknown bark beetles described above and characterized as "Southwest bark beetle complex" in ponderosa pine forests (130 000 ha, 25.1 percent of the total) and fir engraver (59 000 ha, 11.4 percent of the total). Other widespread agents were Douglas-fir beetle (46 000 ha, 8.9 percent) and spruce beetle (*D. rufipennis*) (33 000 ha, 6.4 percent).

A handful of ecoregion sections in the Four Corners region had moderately high mortality density (0.5–2.5 percent of surveyed tree canopy cover) associated with pinyon ips and Southwest bark beetle complex (fig. 2.2). These were 313D–Painted Desert (2.33 percent mortality), 313B–Navajo Canyonlands (1.29 percent), 313A–Grand Canyon (0.83 percent), M313A–White Mountains-San Francisco Peaks-Mogollon Rim (0.64 percent), 313C–Tonto Transition (0.60 percent), and 322A–Mojave Desert (0.53 percent). Several hotspots of moderate mortality density were detected in this area, along with one of high mortality density that was centered on 313B–Navajo Canyonlands in northwestern New Mexico (fig. 2.3).

Finally, surveyors in the Southern FHM megaregion recorded about 13 000 ha of mortality damage attributed to eight mortality agents and complexes in 2022 (table 2.3). Ips engraver beetles were the most widely detected agent, detected on 9000 ha (71.3 percent of the total). Other widespread agents were southern pine beetle (1600 ha, 11.8 percent) and Douglas-fir beetle (1400 ha, 10.5 percent).

Conterminous United States Defoliation

The national IDS database encompassed 59 defoliating agents or complexes across the CONUS in 2022 (table 2.4). These affected approximately 1.87 million ha, which is slightly less than the land area of New Jersey. This continued an upward trend from recent years: 1.54 million ha were attributed to 59 defoliating agents in 2020 and 1.67 million ha were associated with 56 agents in 2021 (Potter and Paschke 2022, 2023). As with 2021, spongy moth was the most widespread defoliation agent in 2022, detected on 707 000 ha or 37.9 percent of the total area of defoliation. Swiss needle cast (caused by the fungus *Nothophaeocryptopus gaeumannii*) was detected on 313 000 ha in Oregon and Washington (16.8 percent of total defoliation) as part of a periodic survey (USDA Forest Service, Pacific Northwest Region 2023). Meanwhile, spruce budworm (*Choristoneura fumiferana*) and western spruce budworm (*C. freemani*) were identified on about 216 000 and 194 000 ha, respectively, or 11.6 and 10.4 percent of the total defoliation area. Forest tent caterpillar (*Malacosoma disstria*) was the only other agent detected on >100 000 ha (114 000 ha, 6.1 percent of the total), but browntail moth (*Euproctis chrysorrhoe*a; 60 000 ha, 3.2 percent) and oak leafroller (*Archips semiferana*; 53 000 ha, 2.8 percent) were also widespread.

Table 2.4—Defoliation agents and complexes affecting >5000 ha in the conterminous United States in 2022

Agents/complexes causing defoliation, 2022	Area (ha)[a]
Spongy moth	706 803
Swiss needle cast	312 770
Spruce budworm	216 426
Western spruce budworm	194 213
Forest tent caterpillar	114 404
Browntail moth	60 075
Oak leafroller	52 535
Unknown defoliator	33 000
Balsam woolly adelgid	30 875
Cytospora canker of fir	27 954
Pinyon needle scale	23 529
Unknown	15 444
Jack pine budworm	12 340
Gelechiid moths/needleminers	12 231
Larch needle cast	12 004
Large aspen tortrix	10 296
Other (43)	36 944
Total, all defoliation agents	1 867 182

[a] All values are "footprint" areas for each agent or complex. The sum of the individual agents is not equal to the total for all agents due to the reporting of multiple agents per polygon.

Surveyors in the Eastern FHM megaregion detected 1.1 million ha of defoliation in 2022 (table 2.5), making this the region with the most defoliation, as in 2021. This encompassed 34 defoliation agents, with spongy moth accounting for almost two-thirds of the defoliated area (697 000 ha). Other widespread defoliators were spruce budworm (216 000 ha, 19.7 percent), browntail moth (60 000 ha, 5.5 percent), and oak leafroller (53 000 ha, 4.8 percent).

Eastern ecoregion sections with the highest levels of defoliation (0.5–10.0 percent of surveyed tree canopy cover) were concentrated in the Great Lakes region (fig. 2.4). Spruce budworm was the main defoliator in 212L–Northern Superior Uplands in northeastern Minnesota (4.8 percent) while spongy moth was the leading defoliation agent in 212H–Northern Lower Peninsula of Michigan (3.4 percent) and adjacent 222J–South Central Great Lakes (0.74 percent). Spongy moth and large aspen tortrix (*Choristoneura conflictana*) were the predominant agents in 212Y–Southwest Lake Superior Clay Plain (in northern Minnesota and Wisconsin and the Upper Peninsula of Michigan), where 9.3 percent of surveyed tree canopy area was affected by defoliation, as well as in neighboring 212J–Southern Superior Uplands (0.8 percent). These two agents, along with forest tent caterpillar, were widespread defoliators in adjacent 212K–Western Superior Uplands in Minnesota and Wisconsin (0.83 percent). Forest tent caterpillar and spruce budworm were the predominant agents in 212S–Northern Upper Peninsula in northern Michigan (2.0 percent), while these two agents along with oak leafroller were the defoliators in 212X–Northern Highlands in northern Wisconsin (0.67 percent). Finally, multiple agents—including spruce budworm, forest tent caterpillar, Chrysomela leaf beetle (*Chrysomela* spp.), and jack pine budworm (*Choristoneura pinus*)—defoliated forests in 212R–Eastern Upper Peninsula of northern Michigan (0.51 percent).

Four of the six CONUS defoliation hotspots for 2022 were identified in the Great Lakes region (fig. 2.5). These were in northern Wisconsin (extremely high and very high defoliation density), in northeastern Minnesota (high defoliation density), and one each in the Lower and Upper Peninsulas of Michigan (moderate defoliation density).

The West Coast FHM megaregion encompassed 397 000 ha of defoliation attributed to 21 agents in 2022 (table 2.5). Most commonly detected was Swiss needle cast, on 313 000 ha, or 78.7 percent of the total defoliation in the region. Balsam woolly adelgid (*Adelges piceae*) was the next most commonly detected, on 31 000 ha (7.8 percent of the total). Cytospora canker of fir (*Cytospora abietis*) was associated with 28 000 ha of defoliation (7.0 percent) and larch needle cast (*Rhabdocline laricis*) with 12 000 ha (3.0 percent).

M242A–Oregon and Washington Coast Ranges experienced high levels of defoliation (3.3 percent of surveyed tree canopy cover), primarily because of Swiss needle cast impacts on Douglas-fir and secondarily because of balsam woolly adelgid damage to several fir species (fig. 2.4). The southern part of this ecoregion, along the coast of Oregon, constituted a hotspot of high defoliation density (fig. 2.5). Two neighboring ecoregion sections (M242B–Western Cascades (0.32

Table 2.5—The top five defoliation agents or complexes for each Forest Health Monitoring megaregion and for Alaska and Hawaii in 2022

Mortality agents and complexes, 2022	Area (ha)[a]
Eastern	
Spongy moth	696 730
Spruce budworm	216 426
Browntail moth	60 075
Oak leafroller	52 535
Forest tent caterpillar	23 869
Other defoliation agents (29)	51 465
Total, all defoliation agents and complexes	1 101 090
Interior West	
Western spruce budworm	194 213
Pinyon needle scale	23 335
Unknown defoliator	23 196
Gelechiid moths/needleminers	12 223
Unknown	3164
Other defoliation agents (15)	7635
Total, all defoliation agents and complexes	263 654
Southern	
Forest tent caterpillar	90 521
Spongy moth	10 073
Fall cankerworm	4489
Baldcypress leafroller	61
Pinyon needle scale	59
Other defoliation agents (1)	37
Total, all defoliation agents and complexes	105 240

Mortality agents and complexes, 2022	Area (ha)[a]
West Coast (CONUS)	
Swiss needle cast	312 770
Balsam woolly adelgid	30 875
Cytospora canker of fir	27 954
Larch needle cast	11 967
Unknown	9835
Other defoliation agents (16)	8336
Total, all defoliation agents and complexes	397 198
Alaska	
Western blackheaded budworm	277 537
Aspen leafminer	15 410
Birch leafminer	8710
Unknown defoliator	6755
Willow leaf blotchminer	6513
Other defoliation agents (2)	824
Total, all defoliation agents and complexes	315 500
Hawaii	
None	0
Total, all defoliation agents and complexes	0

[a] The total area affected by other agents is listed at the end of each section. All values are "footprint" areas for each agent or complex. The sum of the individual agents is not equal to the total for all agents due to the reporting of multiple agents per polygon.

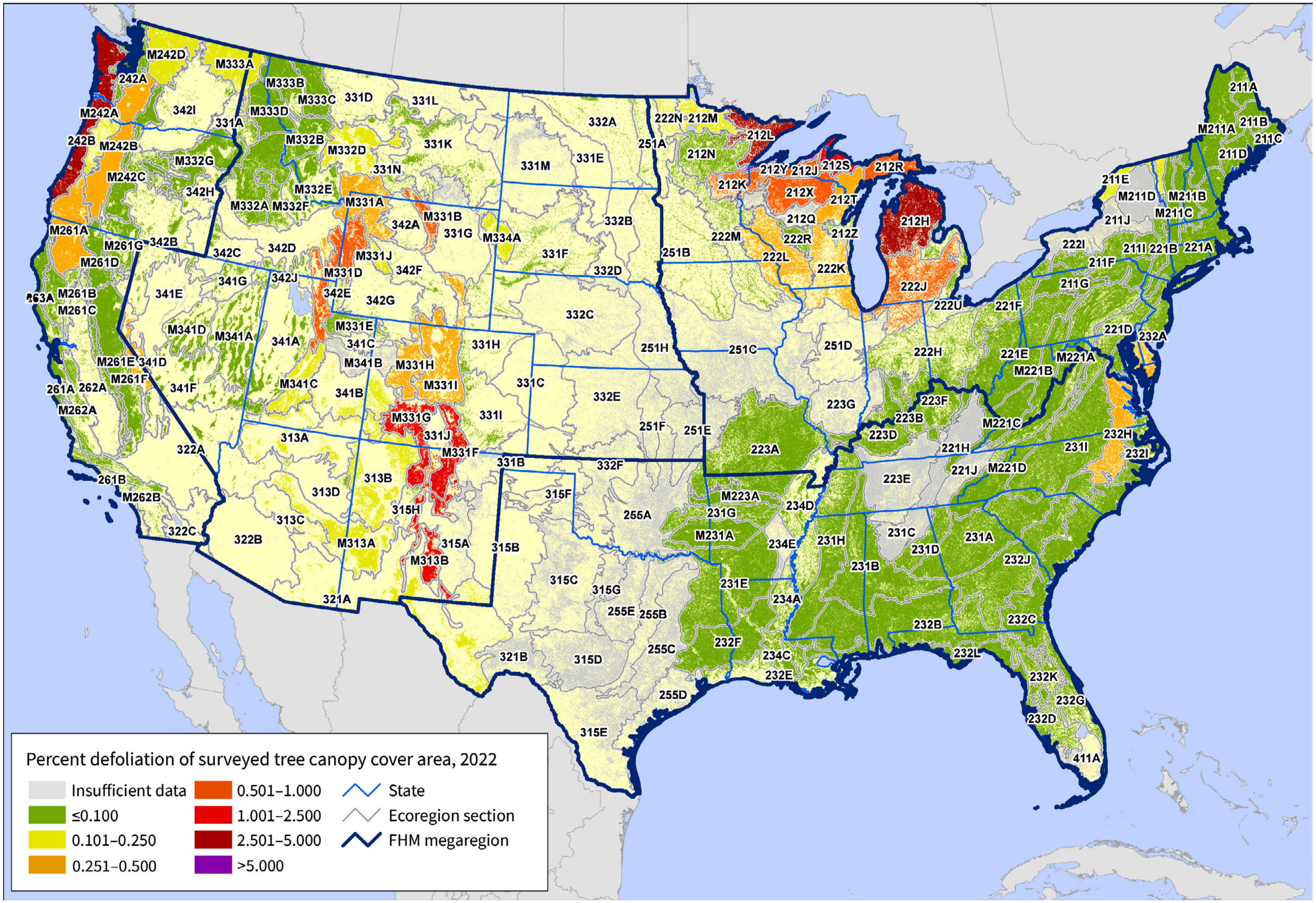

Figure 2.4—The percentage of surveyed tree canopy cover area with insect and disease defoliation, by ecoregion section within the conterminous United States, for 2022. The gray lines delineate ecoregion sections (Cleland and others 2007), and dark blue lines delineate Forest Health Monitoring megaregions. The 240-m tree canopy cover is based on data from a cooperative project between the Multi-Resolution Land Characteristics Consortium (Coulston and others 2012) and the Forest Service Geospatial Technology and Applications Center using the 2011 National Land Cover Database. (Data source: U.S. Department of Agriculture, Forest Service, Forest Health Protection)

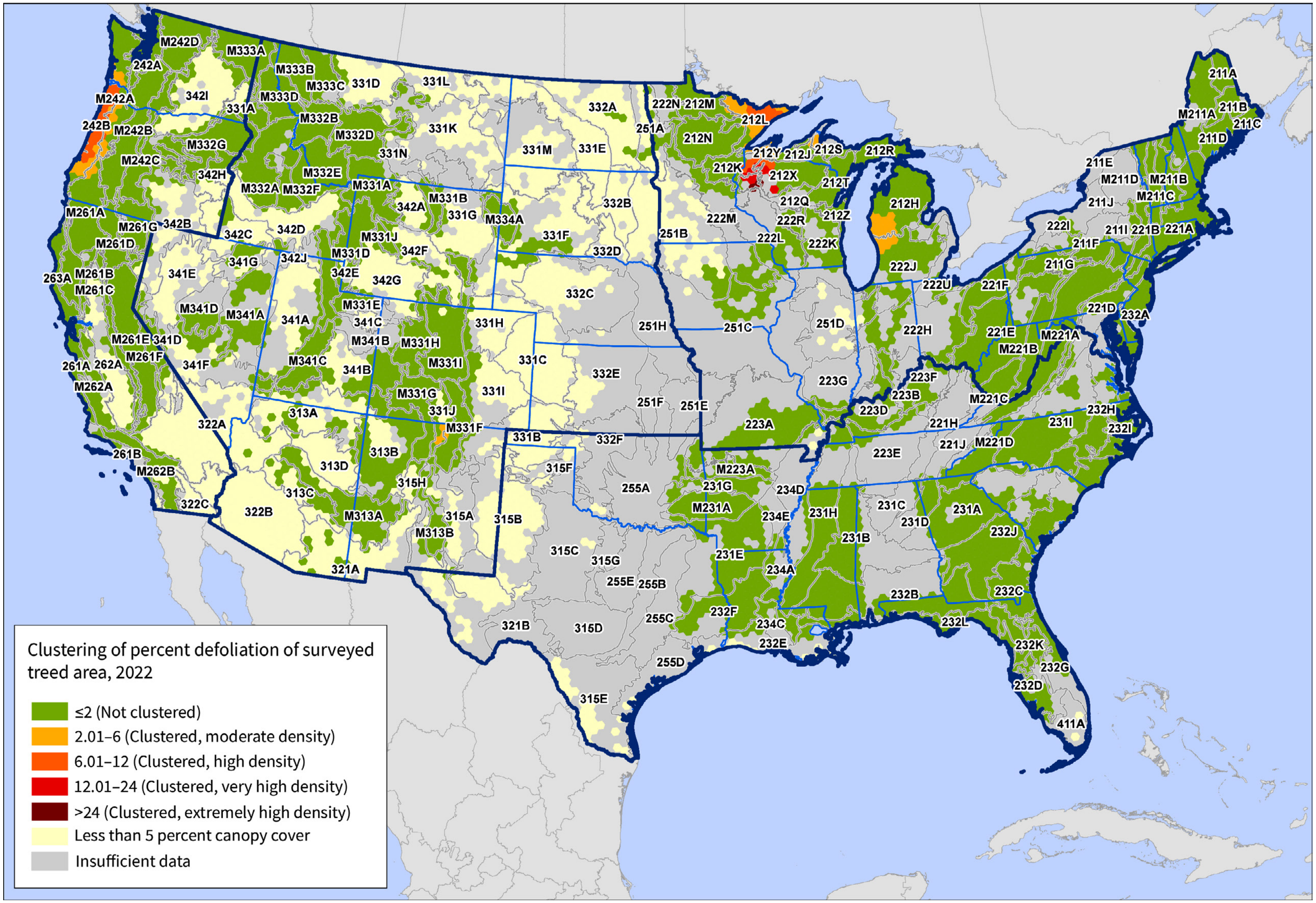

Figure 2.5—Hotspots of percentage of surveyed tree canopy cover area with insect and disease defoliation in 2022 for the conterminous United States by hexagons containing >5 percent tree canopy cover. Values are Getis-Ord Gi scores, with values >2 representing significant clustering of high defoliation occurrence densities. (No areas of significant clustering of low densities, <-2, were detected.) The gray lines delineate ecoregion sections (Cleland and others 2007), and dark blue lines delineate Forest Health Monitoring megaregions. Tree canopy cover is based on data from a cooperative project between the Multi-Resolution Land Characteristics Consortium (Coulston and others 2012) and the Forest Service Geospatial Technology and Applications Center using the 2011 National Land Cover Database. (Data source: U.S. Department of Agriculture, Forest Service, Forest Health Protection)*

percent) and M261A–Klamath Mountains (0.27 percent)) had moderate defoliation caused by Cytospora canker of fir, balsam woolly adelgid, an unknown agent affecting Pacific madrone (*Arbutus menziesii*), and Dothistroma needle blight (*D. septosporum*) in ponderosa pine stands.

Twenty defoliation agents were detected in the Interior West FHM megaregion, affecting 264 000 ha (table 2.5). Western spruce budworm encompassed most (73.7 percent) of this area (194 000 ha), similar to recent years (Potter and Paschke 2022, 2023). Pinyon needle scale (*Matsucoccus acalyptus*) and an unknown defoliator of quaking aspen (*Populus tremuloides*) each affected about 23 000 ha (8.9 percent) while Gelechiid moths/needleminers (*Coleotechnites* spp.) were identified on 12 000 ha (4.6 percent).

The Interior West ecoregion section with the highest percent defoliation of surveyed canopy area (2.1 percent) was M313B–Sacramento-Manzano Mountains in central New Mexico (fig. 2.4), where surveyors detected Douglas-fir tussock moth (*Orgyia pseudotsugata*), pinyon needle scale on twoneedle pinyon (*Pinus edulis*), western spruce budworm, and an unknown defoliator in quaking aspen. Two neighboring ecoregion sections in north-central New Mexico and southern Colorado—M331F–Southern Parks and Rocky Mountain Range (1.9 percent defoliation) and M331G–South-Central Highlands (1.7 percent)—were affected by western spruce budworm, Gelechiid moths/needleminers in ponderosa pine, and the unknown quaking aspen defoliator. This area was the location of the single defoliation hotspot (of moderate density) in the Interior West megaregion (fig. 2.5).

Two ecoregion sections in the central Rocky Mountains of northern Colorado and southern Wyoming experienced moderate levels of defoliation by western spruce budworm and the unknown quaking aspen defoliator: M331I–Northern Parks and Ranges (0.40 percent defoliation of canopy tree cover) and M331H–North-Central Highlands and Rocky Mountains in central Colorado (0.28 percent). Meanwhile, three ecoregion sections to the north were affected by western spruce budworm defoliation:

- M331D–Overthrust Mountains in western Wyoming, southeastern Idaho, and northern Utah (0.63 percent)
- M331B–Bighorn Mountains in north-central Wyoming (0.61 percent)
- M331A–Yellowstone Highlands in northwestern Wyoming and south-central Montana (0.34 percent)

Finally, 341D–Mono in western Nevada had a moderate amount of defoliation (0.35 percent) as a result of pinyon needle scale damage in singleleaf pinyon (*P. monophylla*).

Defoliation detected in the Southern FHM megaregion totaled 105 000 ha, of which 86.0 percent (91 000 ha) was associated with forest tent caterpillar (table 2.5). Other relatively widespread agents were spongy moth (10 000 ha, 9.6 percent) and fall cankerworm (*Alsophila pometaria*; 4000 ha, 4.3 percent). Forest tent caterpillar resulted in a moderate level of defoliation in 232H–Middle Atlantic Coastal Plains and Flatwoods in eastern Virginia and North Carolina (0.33 percent defoliation of surveyed tree canopy cover) (fig. 2.4).

Alaska and Hawaii

In 2022, forest health professionals detected damage from six mortality agents across about 25 000 ha of surveyed Alaskan forest and shrubland (table 2.3). This was a decrease from the 90 000 ha detected in 2021. As in recent previous years, spruce beetle was the most commonly identified agent, detected on 20 000 ha, which represented 79.5 percent of the total mortality damage for the State. The only other relatively widespread agent was yellow-cedar (*Chamaecyparis nootkatensis*) decline, identified on 4700 ha or 19.0 percent of the total. An additional 29 762 ha of 2022 mortality attributed to an unknown defoliator were not included in table 2.3 as this resulted from defoliation that occurred before 2022.

Spruce beetle mortality resulted in moderate to high levels of mortality in ecoregion sections of south-central Alaska (0.5–2.5 percent of surveyed forest and shrubland) (fig. 2.6). In recent years, this area has also experienced a spruce beetle outbreak in stands of white spruce (*Picea glauca*) and black spruce (*P. mariana*) (Potter and Paschke 2022, 2023). This encompassed 133A–Cook Inlet Basin (2.5 percent), M241C–Chugach-St. Elias Mountains (1.0 percent), and M133B–Alaska Range (0.95 percent). Meanwhile, mortality associated with yellow-cedar decline and with an unknown and previously documented (from 2021 or earlier) defoliator in western hemlock (*Tsuga heterophylla*) stands resulted in 0.13 percent mortality of surveyed forest and shrubland of M241D–Alexander Archipelago in the Alaska panhandle.

Alaska in 2022 experienced much more defoliation (about 316 000 ha) than mortality (25 000 ha) (table 2.5). This damage—similar in extent to the previous year and a substantial increase from 2020—was attributed to seven defoliating agents, led by western blackheaded budworm (*Acleris gloverana*), detected on 278 000 ha (88.0 percent of the total damage area). Other much less widely detected defoliation agents were aspen leafminer (*Phyllocnistis populiella*) on 15 000 ha (4.9 percent of the total), birch leafminer (*Fenusa pusilla*) on 9000 ha (2.8 percent), and willow leaf blotchminer (*Micrurapteryx salicifoliella*) on 7000 ha (2.1 percent).

The western blackheaded budworm outbreak in western hemlock, mountain hemlock (*T. mertensiana*), and Sitka spruce (*Picea sitchensis*) caused high levels of defoliation in the Alaska panhandle: 6.8 percent of surveyed forest and shrubland in M241D–Alexander Archipelago and 2.2 percent in M241E–Northern Coast Mountains (fig. 2.7). Meanwhile, the minor agents listed above resulted in moderate levels of defoliation (0.25–1.0) in ecoregion sections of east-central Alaska:

- M132C–Yukon-Tanana Uplands (0.90 percent of surveyed forest and shrubland)
- 132C–Tanana-Kuskokwim Lowlands (0.61 percent)
- 132A–Yukon-Old Crow Basin (0.60 percent)
- M132E–Ray Mountains (0.41 percent)

Additionally, M241B–Gulf Coast of Alaska, along the southern coast of the State, had 0.98 percent defoliation of surveyed forest and shrubland

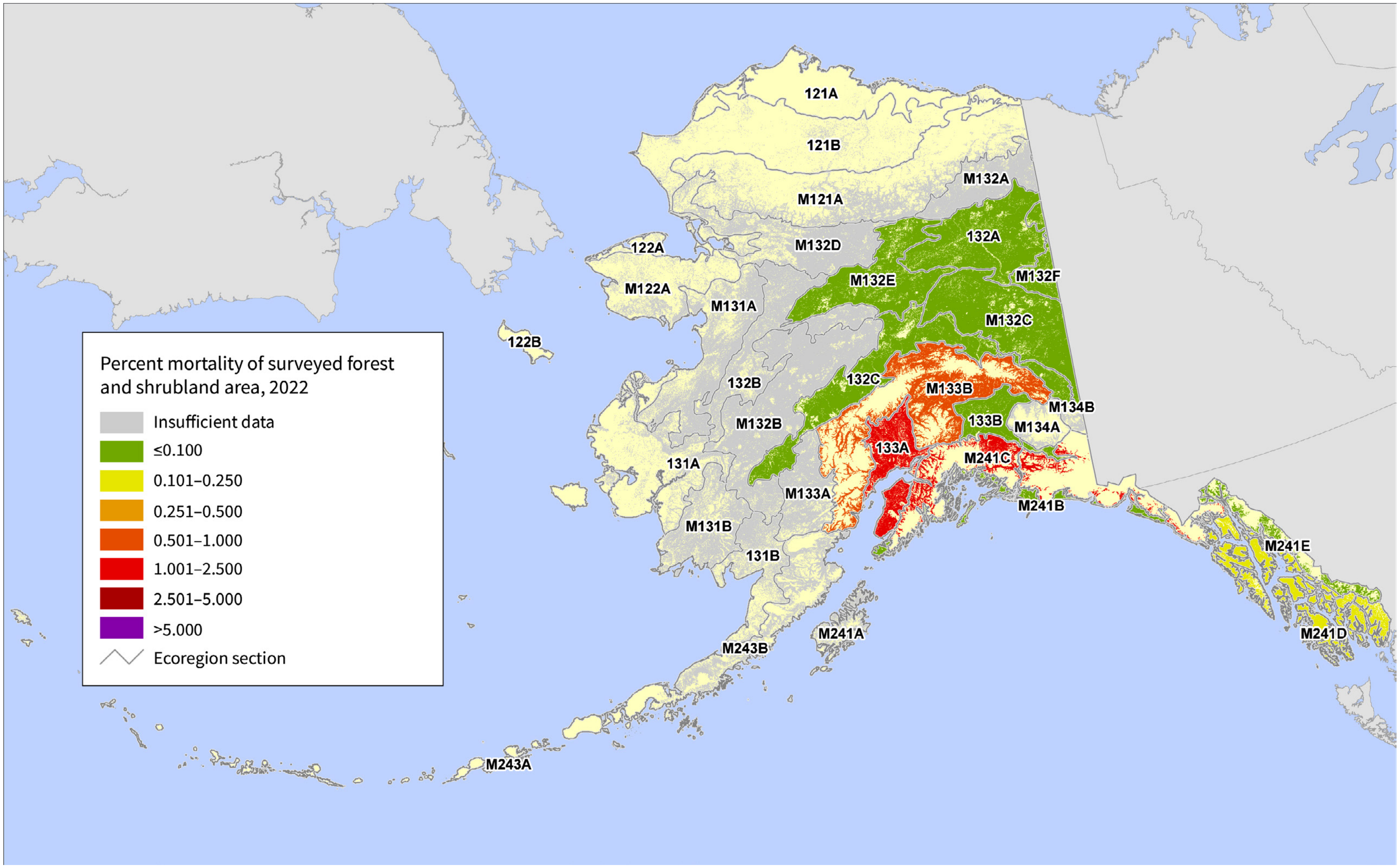

Figure 2.6—Percentage of 2022 surveyed Alaska forest and shrubland area within ecoregions with mortality caused by insects and diseases. The gray lines delineate ecoregion sections (Spencer and others 2002). Forest and shrub cover is derived from the 2011 National Land Cover Database. (Data source: U.S. Department of Agriculture, Forest Service, Forest Health Protection)

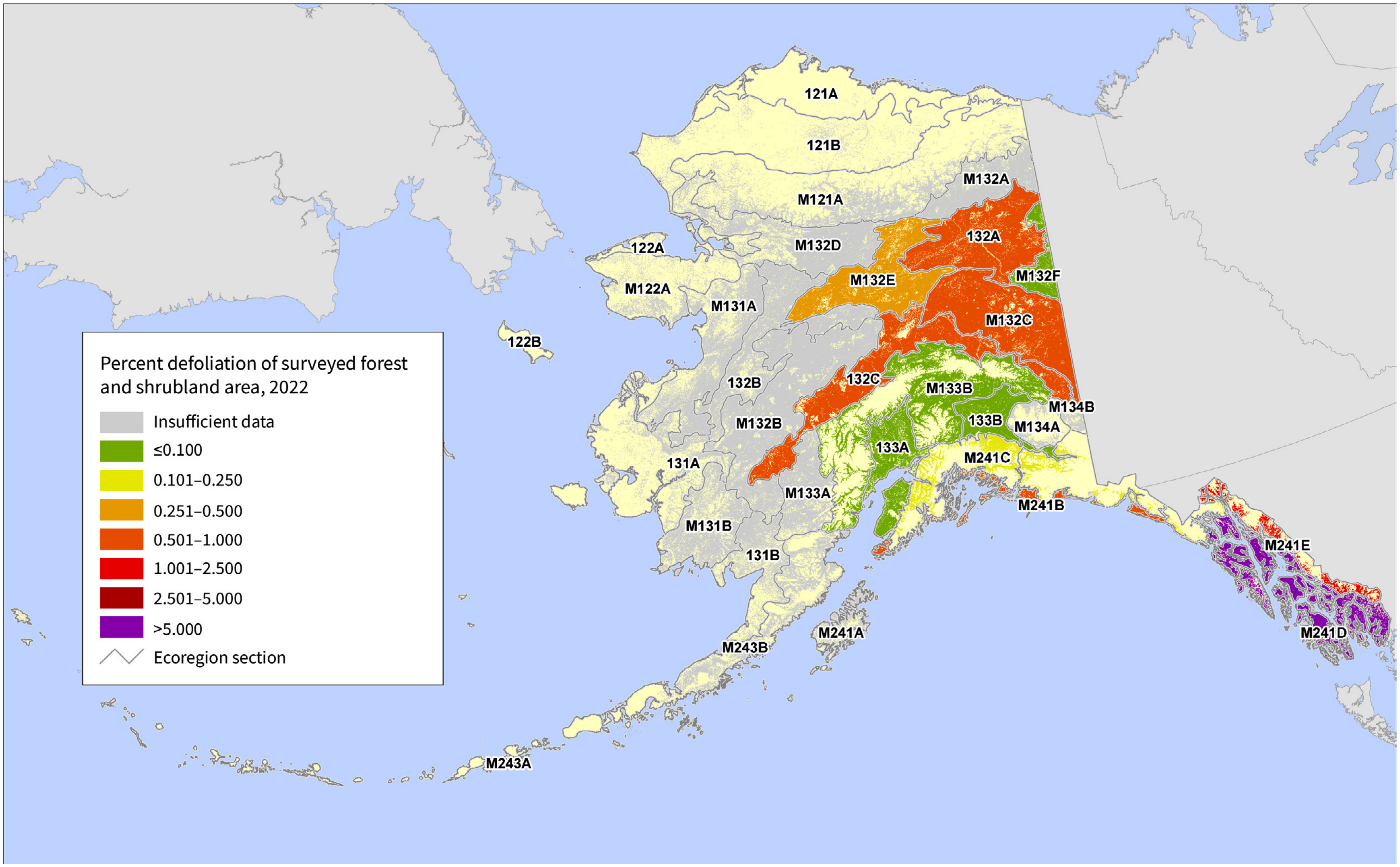

Figure 2.7—Percentage of 2022 surveyed Alaska forest and shrubland area within ecoregions with defoliation caused by insects and diseases. The gray lines delineate ecoregion sections (Spencer and others 2002). Forest and shrub cover is derived from the 2011 National Land Cover Database. (Data source: U.S. Department of Agriculture, Forest Service, Forest Health Protection)

because of an unknown defoliator of alder (*Alnus* spp.) (fig. 2.7).

Finally, in Hawaii, surveyors detected about 36 000 ha of mortality during 2022 (table 2.3), similar to 2021 and an increase compared to 2020 (32 000 ha) and 2019 (27 000 ha) (Potter and Paschke 2022, 2023; Potter and others 2021). The cause of the mortality was designated as "unknown," but at least some of the damage may be the result of rapid ʻōhi'a death, a wilt disease caused by two fungal pathogens—the more aggressive *Ceratocystis lukuohia* and the less aggressive *C. huliohia*—which both can kill ʻōhi'a lehua (*Metrosideros polymorpha*) (Barnes and others 2018). This endemic tree species is the most abundant native tree in Hawaii, where it is deeply woven into Hawaiian culture (University of Hawaiʻi, College of Tropical Agriculture and Human Resources 2023). Both pathogens have been confirmed on Hawai'i Island, where most detections are of the more aggressive C. *lukuohia*, and on Kaua'i Island (University of Hawaiʻi 2023). A small single tree infested with C. *huliohia* was detected and destroyed on Maui in 2019, and about a dozen trees infested with C. *huliohia* have been identified on O'ahu since 2019 (University of Hawaiʻi, College of Tropical Agriculture and Human Resources 2023).

In 2022, mortality was moderate to high (>0.5 percent of surveyed tree canopy cover) across the four montane wet ecoregions of Hawai'i Island (fig. 2.8). This was highest in Montane Wet-Hawai'i-Ka'ū (MWh-ka, 3.3 percent of the surveyed tree canopy area), followed by Montane Wet-Hawai'i-Kona (MWh-ko, 2.2 percent), Montane Wet-Hawai'i-Hilo-Puna (MWh-hp, 1.9 percent), and Montane Wet-Hawai'i-Kohala-Hāmākua (MWh-kh, 0.88 percent). Lower wet and mesic areas of the island had fairly low mortality densities (0.25–0.5 percent). Meanwhile, moderate levels of mortality were detected in the two wet ecoregions on the island of Kaua'i: Lowland Wet-Kaua'i (LWk, 0.74 percent of surveyed tree canopy area) and Montane Wet-Kaua'i (MWk, 0.34 percent).

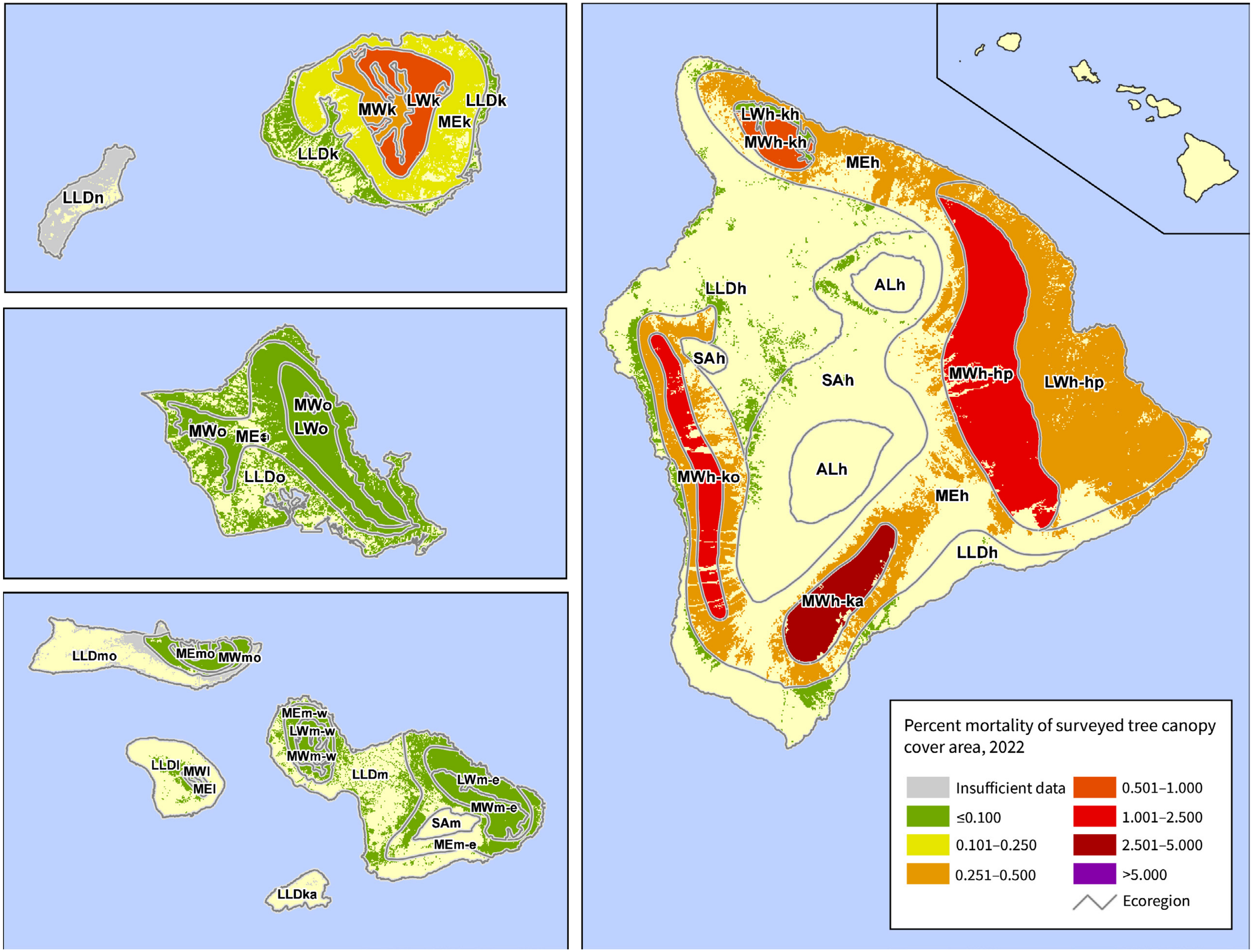

Figure 2.8—Percentage of 2022 surveyed Hawaii tree canopy area within island/ecoregion combinations with mortality caused by insects and diseases. Tree canopy cover is based on data from a cooperative project between the Multi-Resolution Land Characteristics Consortium (Coulston and others 2012) and the Forest Service Geospatial Technology and Applications Center using the 2011 National Land Cover Database. (Data source: U.S. Department of Agriculture, Forest Service, Forest Health Protection)

CONCLUSIONS

Forest health surveyors in 2022 identified 52 mortality-causing agents and complexes on approximately 3.3 million ha across the CONUS, an area similar to that of Connecticut and Massachusetts combined. Fir engraver was the most widely detected mortality agent, identified on about 1.3 million ha in the West Coast FHM megaregion and 59 000 ha in the Interior West megaregion. This is an increase from recent years (e.g., Potter and Paschke 2022, 2023). Emerald ash borer, meanwhile, was detected on about 582 000 ha, mostly in the Eastern megaregion. Alaska experienced mortality from spruce beetle, though less than in recent years, while extensive mortality in Hawaii may be associated with rapid ‘ōhi’a death.

For defoliation, meanwhile, the 2022 national IDS database listed 59 defoliation agents and complexes affecting approximately 1.87 million ha across the CONUS. This area is slightly less than that of New Jersey and continues an upward trend across multiple years (Potter and Paschke 2022, 2023). Spongy moth accounted for a plurality of this area, mostly in the Eastern megaregion but in the Southern megaregion as well. Alaskan forests experienced substantial defoliation as part of an ongoing western blackheaded budworm outbreak in the Alexander Archipelago.

Ongoing, multiple-year monitoring of insect and disease damage across the United States can guide appropriate followup investigation and management activities. The pests and pathogens discussed in this chapter do not include all the biotic forest health threats that are important to be considered when making management decisions and budget allocations, in part because of the limitations of survey efforts to detect certain important forest insects and diseases and to delineate their damage. Despite their shortcomings, large-scale assessments of mortality and defoliation severity represent a constructive approach for identifying geographic areas where monitoring and management activities are most needed and where they might be most effective.

LITERATURE CITED

Abdulridha, J.; Ampatzidis, Y.; Ehsani, R.; de Castro, A.I. 2018. Evaluating the performance of spectral features and multivariate analysis tools to detect laurel wilt disease and nutritional deficiency in avocado. Computers and Electronics in Agriculture. 155: 203–211. https://doi.org/10.1016/j.compag.2018.10.016.

Anselin, L. 1992. Spatial data analysis with GIS: an introduction to application in the social sciences. Tech. Rep. 92-10. Santa Barbara, CA: National Center for Geographic Information and Analysis. 53 p.

Barnes, I.; Fourie, A.; Wingfield, M.J. [and others]. 2018. New *Ceratocystis* species associated with rapid death of *Metrosideros polymorpha* in Hawaii. Persoonia-Molecular Phylogeny and Evolution of Fungi. 40(1): 154–181. https://doi.org/10.3767/persoonia.2018.40.07.

Berryman, E.; McMahan, A. 2019. Using tree canopy cover data to help estimate acres of damage. In: Potter, K.M.; Conkling, B.L., eds. Forest Health Monitoring: national status, trends, and analysis 2018. Gen. Tech. Rep. SRS-239. Asheville, NC: U.S. Department of Agriculture, Forest Service, Southern Research Station: 125–141.

Brockerhoff, E.G.; Liebhold, A.M.; Jactel, H. 2006. The ecology of forest insect invasions and advances in their management. Canadian Journal of Forest Research. 36(2): 263–268. https://doi.org/10.1139/x06-013.

Castello, J.D.; Leopold, D.J.; Smallidge, P.J. 1995. Pathogens, patterns, and processes in forest ecosystems. BioScience. 45(1): 16–24. https://doi.org/10.2307/1312531.

Cleland, D.T.; Freeouf, J.A.; Keys, J.E. [and others]. 2007. Ecological subregions: sections and subsections for the conterminous United States. Gen. Tech. Rep. WO-76D. Washington, DC: U.S. Department of Agriculture, Forest Service. Map; Sloan, A.M., cartographer; presentation scale 1:3,500,000; colored. https://doi.org/10.2737/WO-GTR-76D.

Coleman, T.W.; Graves, A.D.; Heath, Z. [and others]. 2018. Accuracy of aerial detection surveys for mapping insect and disease disturbances in the United States. Forest Ecology and Management. 430: 321–336. https://doi.org/10.1016/j.foreco.2018.08.020.

Coulston, J.W.; Moisen, G.G.; Wilson, B.T. [and others]. 2012. Modeling percent tree canopy cover: a pilot study. Photogrammetric Engineering and Remote Sensing. 78(7): 715–727. https://doi.org/10.14358/PERS.78.7.715.

Edmonds, R.L.; Agee, J.K.; Gara, R.I. 2011. Forest health and protection. Long Grove, IL: Waveland Press, Inc. 667 p.

ESRI. 2017. ArcMap® 10.5.1. Redlands, CA: Environmental Systems Research Institute.

Forest Health Protection (FHP). 2019. Digital Mobile Sketch Mapping user's manual 2.1. Fort Collins, CO: U.S. Department of Agriculture, Forest Service, Forest Health Assessment and Applied Sciences Team. https://www.fs.usda.gov/foresthealth/technology/docs/DMSM_Tutorial/story_content/external_files/DMSM_User_Guide.pdf. [Date accessed: August 10, 2022].

Forest Health Protection (FHP). 2023. Insect and Disease Detection Survey (IDS) data downloads. Fort Collins, CO: U.S. Department of Agriculture, Forest Service, Forest Health Technology Enterprise Team. https://www.fs.usda.gov/science-technology/data-tools-products/fhp-mapping-reporting/detection-surveys. [Date accessed: June 2, 2023].

Getis, A.; Ord, J.K. 1992. The analysis of spatial association by use of distance statistics. Geographical Analysis. 24(3): 189–206. https://doi.org/10.1111/j.1538-4632.1992.tb00261.x.

Hanavan, R.P.; Pontius, J.; Hallett, R. 2015. A 10-year assessment of hemlock decline in the Catskill Mountain region of New York State using hyperspectral remote sensing techniques. Journal of Economic Entomology. 108(1): 339–349. https://doi.org/10.1093/jee/tou015.

Holdenrieder, O.; Pautasso, M.; Weisberg, P.J.; Lonsdale, D. 2004. Tree diseases and landscape processes: the challenge of landscape pathology. Trends in Ecology & Evolution. 19(8): 446–452. https://doi.org/10.1016/j.tree.2004.06.003.

Homer, C.G.; Dewitz, J.A.; Yang, L. [and others]. 2015. Completion of the 2011 National Land Cover Database for the conterminous United States: representing a decade of land cover change information. Photogrammetric Engineering and Remote Sensing. 81(5): 345–354.

Laffan, S.W. 2006. Assessing regional scale weed distributions, with an Australian example using *Nassella trichotoma*. Weed Research. 46(3): 194–206. https://doi.org/10.1111/j.1365-3180.2006.00491.x.

Liebhold, A.M.; McCullough, D.G.; Blackburn, L.M. [and others]. 2013. A highly aggregated geographical distribution of forest pest invasions in the USA. Diversity and Distributions. 19: 1208–1216. https://doi.org/10.1111/ddi.12112.

Logan, J.A.; Regniere, J.; Powell, J.A. 2003. Assessing the impacts of global warming on forest pest dynamics. Frontiers in Ecology and the Envionment. 1: 130–137. https://doi.org/10.1890/1540-9295(2003)001[0130:ATIOGW]2.0.CO;2.

Lovett, G.M.; Weiss, M.; Liebhold, A.M. [and others]. 2016. Nonnative forest insects and pathogens in the United States: impacts and policy options. Ecological Applications. 26: 1437–1455. https://doi.org/10.1890/15-1176.

Mack, R.N.; Simberloff, D.; Lonsdale, W.M. [and others]. 2000. Biotic invasions: causes, epidemiology, global consequences, and control. Ecological Applications. 10(3): 689–710. https://doi.org/10.1890/1051-0761(2000)010[0689:BICEGC]2.0.CO;2.

Manion, P.D. 2003. Evolution of concepts in forest pathology. Phytopathology. 93: 1052–1055. https://doi.org/10.1094/PHYTO.2003.93.8.1052.

Parry, D.; Teale, S.A. 2011. Alien invasions: the effects of introduced species on forest structure and function. In: Castello, J.D.; Teale, S.A., eds. Forest health: an integrated perspective. New York: Cambridge University Press: 115–162. https://doi.org/10.1017/CBO9780511974977.006.

Pontius, J.; Hanavan, R.P.; Hallett, R.A. [and others]. 2017. High spatial resolution spectral unmixing for mapping ash species across a complex urban environment. Remote Sensing of Environment. 199: 360–369. https://doi.org/10.1016/j.rse.2017.07.027.

Potter, K.M. 2012. Large-scale patterns of insect and disease activity in the conterminous United States and Alaska from the national Insect and Disease Detection Survey database, 2007 and 2008. In: Potter, K.M.; Conkling, B.L., eds. Forest Health Monitoring 2009 national technical report. Gen. Tech. Rep. SRS-167. Asheville, NC: U.S. Department of Agriculture, Forest Service, Southern Research Station: 63–78.

Potter, K.M. 2013. Large-scale patterns of insect and disease activity in the conterminous United States and Alaska from the national Insect and Disease Detection Survey, 2009. In: Potter, K.M.; Conkling, B.L., eds. Forest Health Monitoring: national status, trends, and analysis 2010. Gen. Tech. Rep. SRS-176. Asheville, NC: U.S. Department of Agriculture, Forest Service, Southern Research Station: 15–29.

Potter, K.M. 2023. Ecological regions of Hawai'i. Fort Collins, CO: Forest Service Research Data Archive. https://doi.org/10.2737/RDS-2023-0018.

Potter, K.M.; Canavin, J.C.; Koch, F.H. 2020b. A forest health retrospective: national and regional results from 20 years of Insect and Disease Survey data. In: Potter, K.M.; Conkling, B.L., eds. Forest Health Monitoring: national status, trends, and analysis 2019. Gen. Tech. Rep. SRS-250. Asheville, NC: U.S. Department of Agriculture, Forest Service, Southern Research Station: 125–149.

Potter, K.M.; Escanferla, M.E.; Jetton, R.M.; Man, G. 2019a. Important insect and disease threats to United States tree species and geographic patterns of their potential impacts. Forests. 10(4): 304. https://doi.org/10.3390/f10040304.

Potter, K.M.; Escanferla, M.E.; Jetton, R.M. [and others]. 2019b. Prioritizing the conservation needs of United States tree species: evaluating vulnerability to forest insect and disease threats. Global Ecology and Conservation. 18: e00622. https://doi.org/10.1016/j.gecco.2019.e00622.

Potter, K.M.; Koch, F.H. 2012. Large-scale patterns of insect and disease activity in the conterminous United States and Alaska, 2006. In: Potter, K.M.; Conkling, B.L., eds. Forest Health Monitoring 2008 national technical report. Gen. Tech. Rep. SRS-158. Asheville, NC: U.S. Department of Agriculture, Forest Service, Southern Research Station: 63–72. https://doi.org/10.2737/SRS-GTR-158.

Potter, K.M.; Koch, F.H.; Oswalt, C.M.; Iannone, B.V. 2016. Data, data everywhere: detecting spatial patterns in fine-scale ecological information collected across a continent. Landscape Ecology. 31: 67–84. https://doi.org/10.1007/s10980-015-0295-0.

Potter, K.M.; Paschke, J.L. 2013. Large-scale patterns of insect and disease activity in the conterminous United States and Alaska from the national Insect and Disease Detection Survey database, 2010. In: Potter, K.M.; Conkling, B.L., eds. Forest Health Monitoring: national status, trends, and analysis 2011. Gen. Tech. Rep. SRS-185. Asheville, NC: U.S. Department of Agriculture, Forest Service, Southern Research Station: 15–28.

Potter, K.M.; Paschke, J.L. 2014. Large-scale patterns of insect and disease activity in the conterminous United States and Alaska from the national Insect and Disease Survey database, 2011. In: Potter, K.M.; Conkling, B.L., eds. Forest Health Monitoring: national status, trends, and analysis 2012. Gen. Tech. Rep. SRS-198. Asheville, NC: U.S. Department of Agriculture, Forest Service, Southern Research Station: 19–34.

Potter, K.M.; Paschke, J.L. 2015a. Large-scale patterns of insect and disease activity in the conterminous United States and Alaska from the national Insect and Disease Survey, 2012. In: Potter, K.M.; Conkling, B.L., eds. Forest Health Monitoring: national status, trends, and analysis 2013. Gen. Tech. Rep. SRS-207. Asheville, NC: U.S. Department of Agriculture, Forest Service, Southern Research Station: 19–36.

Potter, K.M.; Paschke, J.L. 2015b. Large-scale patterns of insect and disease activity in the conterminous United States, Alaska, and Hawaii from the national Insect and Disease Survey, 2013. In: Potter, K.M.; Conkling, B.L., eds. Forest Health Monitoring: national status, trends, and analysis 2014. Gen. Tech. Rep. SRS-209. Asheville, NC: U.S. Department of Agriculture, Forest Service, Southern Research Station: 19–38.

Potter, K.M.; Paschke, J.L. 2016. Large-scale patterns of insect and disease activity in the conterminous United States and Alaska from the national Insect and Disease Survey, 2014. In: Potter, K.M.; Conkling, B.L., eds. Forest Health Monitoring: national status, trends, and analysis 2015. Gen. Tech. Rep. SRS-213. Asheville, NC: U.S. Department of Agriculture, Forest Service, Southern Research Station: 21–40.

Potter, K.M.; Paschke, J.L. 2017. Large-scale patterns of insect and disease activity in the conterminous United States and Alaska from the national Insect and Disease Survey, 2015. In: Potter, K.M.; Conkling, B.L., eds. Forest Health Monitoring: national status, trends, and analysis 2016. Gen. Tech. Rep. SRS-222. Asheville, NC: U.S. Department of Agriculture, Forest Service, Southern Research Station: 21–42.

Potter, K.M.; Paschke, J.L. 2022. Broad-scale patterns of insect and disease activity across the 50 United States from the national Insect and Disease Survey, 2020. In: Potter, K.M.; Conkling, B.L., eds. Forest Health Monitoring: national status, trends, and analysis, 2021. Gen. Tech. Rep. SRS-266. Asheville, NC: U.S. Department of Agriculture, Forest Service, Southern Research Station: 25–49. https://doi.org/10.2737/SRS-GTR-266-Chap2.

Potter, K.M.; Paschke, J.L. 2023. Broad-scale patterns of insect and disease activity across the United States from the national Insect and Disease Survey, 2021. In: Potter, K.M.; Conkling, B.L., eds. Forest Health Monitoring: national status, trends, and analysis, 2022. Gen. Tech. Rep. SRS-273. Asheville, NC: U.S. Department of Agriculture, Forest Service, Southern Research Station: 25–53. https://doi.org/10.2737/SRS-GTR-273-Chap2.

Potter, K.M.; Paschke, J.L.; Koch, F.H.; Berryman, E.M. 2020a. Large-scale patterns of insect and disease activity in the conterminous United States, Alaska, and Hawaii from the national Insect and Disease Survey, 2018. In: Potter, K.M.; Conkling, B.L., eds. Forest Health Monitoring: national status, trends, and analysis 2019. Gen. Tech. Rep. SRS-250. Asheville, NC: U.S. Department of Agriculture, Forest Service, Southern Research Station: 27–55.

Potter, K.M.; Paschke, J.L.; Koch, F.H.; Zweifler, M. 2019c. Large-scale patterns of insect and disease activity in the conterminous United States, Alaska, and Hawaii from the national Insect and Disease Survey, 2017. In: Potter, K.M.; Conkling, B.L., eds. Forest Health Monitoring: national status, trends, and analysis 2018. Gen. Tech. Rep. SRS-239. Asheville, NC: U.S. Department of Agriculture, Forest Service, Southern Research Station: 21–49.

Potter, K.M.; Paschke, J.L.; Berryman, E.M. 2021. Large-scale patterns of insect and disease activity in the conterminous United States, Alaska, and Hawaii from the national Insect and Disease Survey, 2019. In: Potter, K.M.; Conkling, B.L., eds. Forest Health Monitoring: national status, trends, and analysis 2020. Gen. Tech. Rep. SRS-261. Asheville, NC: U.S. Department of Agriculture, Forest Service, Southern Research Station: 27–57.

Potter, K.M.; Paschke, J.L.; Zweifler, M. 2018. Large-scale patterns of insect and disease activity in the conterminous United States, Alaska, and Hawaii from the national Insect and Disease Survey, 2016. In: Potter, K.M.; Conkling, B.L., eds. Forest Health Monitoring: national status, trends, and analysis 2017. Gen. Tech. Rep. SRS-233. Asheville, NC: U.S. Department of Agriculture, Forest Service, Southern Research Station: 23–44.

Reams, G.A.; Smith, W.D.; Hansen, M.H. [and others]. 2005. The Forest Inventory and Analysis sampling frame. In: Bechtold, W.A.; Patterson, P.L., eds. The enhanced Forest Inventory and Analysis Program—national sampling design and estimation procedures. Asheville, NC: U.S. Department of Agriculture, Forest Service, Southern Research Station: 11–26.

Shima, T.; Sugimoto, S.; Okutomi, M. 2010. Comparison of image alignment on hexagonal and square lattices. In: 2010 IEEE international conference on image processing. [Place of publication unknown]: Institute of Electrical and Electronics Engineers, Inc.: 141–144. https://doi.org/10.1109/icip.2010.5654351.

Slaton, M.R.; Warren, K.; Koltunov, A.; Smith, S. 2021. Accuracy assessment of Insect and Disease Survey and eDART for monitoring forest health. In: Potter, K.M.; Conkling, B.L., eds. Forest Health Monitoring: national status, trends, and analysis 2020. Gen. Tech. Rep. SRS-261. Asheville, NC: U.S. Department of Agriculture, Forest Service, Southern Research Station: 187–195.

Spencer, P.; Nowacki, G.; Fleming, M. [and others]. 2002. Home is where the habitat is: an ecosystem foundation for wildlife distribution and behavior. Arctic Research of the United States. 16: 6–17.

Teale, S.A.; Castello, J.D. 2011. Regulators and terminators: the importance of biotic factors to a healthy forest. In: Castello, J.D.; Teale, S.A., eds. Forest health: an integrated perspective. New York: Cambridge University Press: 81–114. https://doi.org/10.1017/CBO9780511974977.005.

Tobin, P.C. 2015. Ecological consequences of pathogen and insect invasions. Current Forestry Reports. 1: 25–32. https://doi.org/10.1007/s40725-015-0008-6.

University of Hawai'i, College of Tropical Agriculture and Human Resources. 2023. Rapid 'ōhi'a death. http://rapidohiadeath.org. [Date accessed: June 13, 2023].

U.S. Department of Agriculture (USDA), Forest Service, Pacific Northwest Region. 2023. Forest health highlights in Oregon - 2022. https://www.fs.usda.gov/science-technology/data-tools-products/fhp-mapping-reporting/detection-surveys. [Date accessed: November 8, 2024].

White, D.; Kimerling, A.J.; Overton, W.S. 1992. Cartographic and geometric components of a global sampling design for environmental monitoring. Cartography and Geographic Information Systems. 19(1): 5–22. https://doi.org/10.1559/152304092783786636.

Zhang, L.; Rubin, B.D.; Manion, P.D. 2011. Mortality: the essence of a healthy forest. In: Castello, J.D.; Teale, S.A., eds. Forest health: an integrated perspective. New York: Cambridge University Press: 17–49. https://doi.org/10.1017/CBO9780511974977.003.